10-2015

Activation of Toll-like Receptor 4 (TLR4) Attenuates Adaptive Thermogenesis via Endoplasmic Reticulum Stress

Meshail Okla
University of Nebraska–Lincoln

Wei Wang
University of Nebraska–Lincoln

Inhae Kang
University of Nebraska–Lincoln

Anjeza Pashaj
University of Nebraska–Lincoln

Timothy P. Carr
University of Nebraska - Lincoln, tcarr2@unl.edu

See next page for additional authors

Published in *The Journal of Biological Chemistry* 290:44 (October 30, 2015), pp. 26476–26490. doi 10.1074/jbc.M115.677724

Submitted July 9, 2015; revised September 7, 2015; published online September 14, 2015.

Activation of Toll-like Receptor 4 (TLR4) Attenuates Adaptive Thermogenesis via Endoplasmic Reticulum Stress

Meshail Okla, Wei Wang, Inhae Kang, Anjeza Pashaj, Timothy Carr, and Soonkyu Chung

Department of Nutrition and Health Sciences, University of Nebraska–Lincoln, Lincoln, Nebraska 68583

Corresponding author — S. Chung, Dept. of Nutrition and Health Sciences, University of Nebraska–Lincoln, 316G Ruth Leverton Hall, P. O. Box 830806, Lincoln, NE 68583; tel 402-472-7689, fax 402-472-1587, email schung4@unl.edu

Background: Human obesity is associated with defective brown adipose tissue (BAT) activation.
Results: Toll-like receptor 4(TLR4) activation by high fat diet or lipopolysaccharide impairs adaptive thermogenesis.
Conclusion: Obesity-mediated TLR4 activation represses adaptive thermogenesis through endoplasmic reticulum (ER) stress-mediated mitochondrial dysfunction.
Significance: Inhibition of TLR4/ER stress axis is a novel target to augment BAT activity.

Abstract

Adaptive thermogenesis is the cellular process transforming chemical energy into heat in response to cold. A decrease in adaptive thermogenesis is a contributing factor to obesity. However, the molecular mechanisms responsible for the compromised adaptive thermogenesis in obese subjects have not yet been elucidated. In this study we hypothesized that Toll-like receptor 4 (TLR4) activation and subsequent inflammatory responses are key regulators to suppress adaptive thermogenesis. To test this hypothesis, C57BL/6 mice were either fed a palmitate-enriched high fat diet or administered with chronic low-dose LPS before cold acclimation. TLR4 stimulation by a high fat diet or LPS were both associated with reduced core body temperature and heat release. Impairment of thermogenic activation was correlated with diminished expression of brown-specific markers and mitochondrial dysfunction in subcutaneous white adipose tissue (sWAT). Defective sWAT browning was concomitant with elevated levels of endoplasmic reticulum (ER) stress and autophagy. Consistently, TLR4 activation by LPS abolished cAMP-induced upregulation of uncoupling protein 1 (UCP1) in primary human adipocytes, which was reversed by silencing of C/EBP homologous protein (CHOP). Moreover, the inactivation of ER stress by genetic deletion of CHOP or chemical chaperone conferred a resistance to the LPS-induced suppression of adaptive thermogenesis. Collectively, our data indicate the existence of a novel signaling network that links TLR4 activation, ER stress, and mitochondrial dysfunction, thereby antagonizing thermogenic activation of sWAT. Our results also suggest that TLR4/ER stress axis activation may be a responsible mechanism for obesity-mediated defective brown adipose tissue activation.

There are three distinct types of adipocytes: white, beige, and classical brown. White adipocytes store energy in the form of triglycerides, whereas beige and brown adipocytes dissipate energy in the form of heat via uncoupling protein 1 (UCP1) (1). UCP1 mediates non-shivering thermogenesis by generating heat through a futile cycle of proton transport across the inner mitochondrial membrane. Classical brown adipocytes originate from a myogenic lineage ($Myf5^+$) and possess a constitutively active UCP1 expression (2). Conversely, beige adipocytes are differentiated from the non-myogenic lineage progenitors ($Myf5^-$) and have low levels of UCP1 expression at unstimulated states. However, the ultimate thermogenic function of stimulated-beige adipocytes is indistinguishable from that of classical brown adipocytes (3).

The appearance of beige adipocytes within white adipose tissue (WAT) depots is so-called "WAT browning." The name is derived from the distinctive brown color that occurs due to an increase of iron associated with a high number of mitochondria in the cells (4). Studies in rodents showed that beige adipocytes are flexible for browning and whitening (reversal of browning) (5, 6). This implies there is a regulatory signaling that switches the dynamics of mitochondria back and forth to coordinate heat generation in the presence and absence of thermogenic cues. Despite some controversies surrounding transdifferentiation of white to beige adipocytes (or vice versa), the metabolic significance of beige adipocytes has been well established in humans (7, 8).

Recent research using ^{18}F-2-deoxy-glucose-positron emission tomography (^{18}FDG-PET) has revealed that adult humans possess a substantial amount of functional BAT (mostly beige adipocytes) upon cold exposure (9, 10). These studies suggest that BATs are key metabolic sites to dispose of glucose and fatty ac-

Abbreviations: UCP1, uncoupling protein 1; ER, endoplasmic reticulum; CHOP, C/EBP homologous protein; WAT, white adipose tissue; sWAT subcutaneous WAT; BAT, brown adipose tissue; iBAT, interscapular BAT; TLR4, toll-like receptor 4; PA, palmitate; HF, high fat; PBA, sodium 4-phenybutyrate; Bt_2cAMP, dibutyryl-cAMP; Tg, thapsigargin; LF, low fat; EMSC, ear mesenchymal stem cells; ROS, reactive oxygen species; DCFDA, 2,7-dichlorodihydro-fluorescein diacetate; q-PCR, quantitative PCR; VDAC, voltage-dependent anion channel; PDH, pyruvate dehydrogenase; ANOVA, analysis of variance; Atg5, autophagy-related 5.

ids (11). Thus, the augmentation of BAT activity is receiving extensive attention as a possible therapeutic target to counteract weight gain and metabolic complications. Apparently, however, WAT browning is not equally active in all humans. BAT mass or activity is inversely associated with body mass index, fasting glucose levels, and aging (10), suggesting that metabolic stresses impair WAT browning and thermogenesis.

Diet-induced obesity is associated with ER stress (12, 13) and chronic low-grade inflammation (also called meta-inflammation) (14–16). It has been clearly demonstrated that activation of toll-like receptor 4 (TLR4) by fatty acids, especially palmitate (PA) is a key mediator linking high fat (HF) diet-mediated inflammatory responses to the pathogenesis of obesity and insulin resistance (17). Inactivation of TLR4 by genetic deletion or loss of function mutation reversed HF-mediated body gain and ameliorated metabolic dysfunctions (18–20). Also, Pierre *et al.* (19) have reported that TLR4 knockout confers a resistance against HF diet-induced ER stress in mice. Despite the critical contribution of TLR4/ER stress to obesity and metabolic dysfunction, it is unknown whether TLR4 signaling *per se* or TLR4/ER stress signaling circuit could impede WAT browning and thermogenesis.

The objective of this study was to identify the signaling crosstalk by which obesity and inflammation interfere with WAT browning and thermogenesis. In this study we simulated inflammatory conditions of obesity and insulin resistance by using two separate experimental settings of TLR4 stimulation and assessed the metabolic adaptation to cold in terms of white to beige adipocyte conversion. Here we report for the first time that TLR4/ER axis activation represses WAT browning via mitochondrial dysfunction.

Experimental Procedures

Chemicals—Fetal bovine serum was purchased from Gibco. Rosiglitazone and sodium 4-phenybutyrate (PBA) were purchased from Cayman Chemical. Lipopolysaccharides (LPS) from *Escherichia coli* 055:B5 (3×10^6 endotoxin units/mg), dibutyryl (Bt_2) cAMP, thapsigargin (Tg), insulin, 3-isobutyl-1-methylxanthine, and chloroquine diphosphate salt were purchased from Sigma.

Animals—All protocols and procedures were approved by the Institutional Animal Care and Use Committee at the University of Nebraska-Lincoln. C57BL/6 male mice were purchased at 8 weeks of age from The Jackson Laboratory. For diet-induced TLR4 activation, mice were randomly assigned into two groups receiving either a low fat (LF; 10% calories from fat) diet or a HF (50% calories from fat) diet (n = 24 per group). The AIN-93G rodent formulation was modified for fat composition, and fatty acid profiles were analyzed by GC (data not shown). After 12 weeks of supplementation at ambient temperature (25 °C), ⅓ of the mice of each group (n = 8) were housed at 25 °C. The remaining mice were exposed to 8 °C for either acute-cold treatment for 75 min or chronic-cold treatment for an additional 2 weeks (Fig. 1*A*). During the cold acclimation period, mice were fed the same diet. For LPS-mediated TLR4 activation, C57BL/6 male mice were divided into two groups and housed at either 25 °C ambient temperature (n = 16) or 8 °C (n = 16) for 2 weeks. In both temperature settings, mice received either saline or *E. coli* LPS for TLR4 activation. Approximately, 100 μl of PBS or LPS (7.5 μg/mouse, equivalent to 225,000 endotoxin units) dissolved in saline was administered intraperitoneally every other day. Another set of mice (n = 16) were first treated with either saline or LPS for 2 weeks at ambient temperature then exposed to 8 °C cold for 75 min (Fig. 2*A*). For chemical inhibition of ER stress, C57BL/6 mice received daily injections of PBA, an average dose of 200 mg/kg/day.

The homozygous knock-out for TLR4 expression ($TLR4^{-/-}$, B6.B10ScN-$Tlr4^{lps\text{-}del}$/JthJ) and C/EBP homologous protein ($CHOP^{-/-}$, B6.129 (Cg)-$Ddit3^{tm2.1Dron}$/J) were purchased from The Jackson Laboratory and bred at ambient temperature. For cold acclimation, $CHOP^{-/-}$ and $TLR4^{-/-}$ were housed at 8 °C with or without LPS administration every other day for 2 weeks (n = 6–7 per group). At the time of necropsy, blood, subcutaneous (inguinal), epididymal, and interscapular brown fat were collected, snap-frozen in liquid nitrogen, and kept at –80 °C until analysis.

Blood Sample Analysis—Fasting (6 h) blood glucose levels (mg/dl) were measured using a glucometer (Contour, Bayer). Commercial ELISA kits were used to determine plasma levels of insulin (Crystal Chem) and adiponectin (R&D Systems). Plasma cholesterol was determined with an enzymatic colorimetric assay kit (Roche Applied Science).

Rectal Temperature and Thermogenesis—To measure core body temperature, a digital thermometer (TC Thermocouple Meter) was used in combination with a copper thermocouple rectal probe (RET-3) (Kent Scientific Corp). The probe was properly positioned into the anal ducts of adult mice to record temperature. An average of three readings obtained from the same mouse was calculated. For the detection of thermal release, an infrared (IR) camera (A655sc, FLIR Systems) was used to acquire images of body surface temperature of each mouse. Images were displayed using the rainbow high contrast color palette in the FLIR Research IR program using a temperature linear display between 25 and 34 °C. Mean surface temperature in Fig. 6*H* was calculated by following the method of Crane *et al.* (21).

Preparation and Treatment of Primary Cultures of Adipocytes— To prepare the primary cultures of human adipocytes, abdominal adipose tissues were obtained from females with a body mass index of ~30 kg/m^2 during liposuction or abdominoplastic surgery. All protocols and procedures were approved by the Institutional Review Board at the University of Nebraska–Lincoln. Isolation of human adipose-derived stem cells (*h*ASCs), and differentiation of adipocytes was conducted as we described previously (22). To prepare the primary cultures of rodent adipocytes, ear mesenchymal stem cells (EMSC) were prepared from ears of wild-type, $CHOP^{-/-}$, and $TLR4^{-/-}$ mice (23). Briefly, EMSC were isolated from the pools of 3–8 ears from adult mice (n = 3–4) by collagenase digestion (2 mg/ml). The confluent cultures of EMSC were stimulated with adipogenic differentiation mixture according to standard adipocyte differentiation protocols (24). For LPS treatment, adipocyte cultures were incubated with LPS (100 ng/ml) for 72 h followed by dibutyryl cAMP (Bt_2cAMP; 0.5mM) for 6–12 h. To deplete C/EBP homologous protein (CHOP) in cultures of human adipocytes, siRNAs (On-Target smart pool) targeting to human CHOP (DDIT3) were transfected with a final concentration of 100 nM using DharmaFECT1 trans-

fection reagent (GE Healthcare). After 48 h post-transfection, cells were washed and used for experiments (Fig. 5, *I* and *J*).

Oxygen Consumption Rate—Adipocytes were grown in a 96-well clear-bottom black polystyrene sterile plate (Corning). To determine the stimulated levels of oxygen consumption, cells were incubated with 1 mM Bt_2cAMP for 6 h. Oxygen consumption rate was determined using MitoXpress® (Cayman Chemical) according to the manufacturer's protocol. Briefly, an increase of phosphorescent signal from the oxygen-sensitive probe in the medium was measured every 3 min over 5 h using a Synergy H1 multi-mode microplate reader (BioTek).

Cellular Reactive Oxygen Species (ROS) Production—To measure intracellular accumulation of ROS), a commercial kit of DCFDA (2,7-dichloro-dihydro-fluorescein diacetate) cellular ROS detection (Cayman) was used following the manufacturer's protocol. Oxidation of DCFDA to the highly fluorescent 2,7-dichlorofluorescein (DCF) was proportionate to ROS generation, and fluorescence intensity was measured by Synergy H1.

qPCR—Total RNA was extracted using TRIzol® reagent (Invitrogen) from homogenized tissues/cells according to the manufacturer's instructions. RNA was purified using DNase (5 PRIME). 2 μg of RNA was converted into cDNA (iScript, Bio-Rad). Relative gene expression was determined based on the $2^{-\Delta\Delta CT}$ method with normalization of the raw data to either 36B4 or GAPDH (primer sequences are available upon request).

mtDNA Quantification by qPCR—Selected mouse tissues were homogenized, and genomic DNA was isolated using DNAzol (Life Technologies). Quantitative PCR was performed in duplicate using mtDNA specific primer (16S rRNA) and nuclear-specific PCR (hexokinase 2) using the published primer sequences by Lagouge *et al.* (25). Results were calculated from the difference in threshold cycle values for mtDNA and nuclear specific amplification.

Western Blot Analysis—Tissue and cell extracts were prepared as previously described (22). Proteins were fractionated using 4–15% precast polyacrylamide gel (Bio-Rad) and transferred to PVDF membranes with a semi-dry transfer unit (Hoefer TE77X). Antibodies against voltage-dependent anion channels (VDAC; 4661), pyruvate dehydrogenase (PDH; 3205), cytochrome *c* (4280), β-actin (4967), CHOP (2895), Beclin1 (3738), BiP (3183), p-JNK (4668), LC3 (2775), and autophagy-related 5 (Atg5; D1G9) were obtained from Cell Signaling Technology. Antibody against p62 (ab56416) was purchased from Abcam, and UCP1 (sc-6528) was purchased from Santa Cruz Biotechnology. Antibodies against apoA1 (K23500R) and apoB (K23300R) were obtained from Life Sciences. Blots were visualized with FluorChem™ E imaging system (Protein Simple).

Hematoxylin and Eosin (H&E) Staining—Adipose tissue samples (inguinal, epididymal, and interscapular brown fat) were fixed immediately in 10% buffered formalin. Paraffin-embedded adipose tissues were sectioned into 10-μm thickness for H&E staining.

Statistical Analysis—All data are presented as the means ±S.E. Independent samples were statistically analyzed using Student's *t* test or one-way ANOVA followed by Tukey's multiple comparison tests for comparisons between two groups. Two-way ANOVA with repeated measures (time course, 0–60 min) was used to determine the effects of CHOP deletion on LPS-inducible ROS production by assessing the differences in ROS production between LPS-treated adipocytes and wild-type adipocytes without LPS (control) (Bonferroni's multiple test) (Fig. 6*C*). All statistical analyses were conducted by Graph Pad Prism 6 (Version 6.02).

Results

TLR4 Activation by HF Diet-impaired Thermogenesis—To investigate the impact of diet-induced TLR4 activation on thermogenic potential, C57BL/6 mice were fed with either LF diet (10% calories from fat) or HF diet (50% calories from fat) for 12 weeks at ambient temperature followed by another 2 weeks at 8 °C (Fig. 1*A*). Total calorie consumption per day (calorie/g diet × daily consumption) was not different between diet groups (Fig. 1*B*, *left*). However, calorie consumption from the PA was ~10-fold higher in HF-fed mice (3.33 kcal of PA/day) than LF-fed mice (0.39 kcal PA/day). As we expected, HF diet was associated with increased body weight (Fig. 1*B*, *right*) and elevated fasting glucose levels (Fig. 1*C*). TLR4 activation was confirmed by qPCR. Consistent with the previous publication (17), chronic feeding of a HF diet enriched with PA significantly increased (~1.5-fold) TLR4 gene expression compared with LF diet (Fig. 1*D*). There was no difference between LF- and HF-fed mice in either the core body temperature measured (as measured by a rectal thermometer; Fig. 1*E*) or UCP1 gene expression of interscapular brown fat (iBAT) at 25 °C. Interestingly, PRDM16 gene expression was significantly lower in mice fed an HF diet even at ambient temperature (Fig. 1*F*). When exposed to 8 °C acutely (for 75 min), core body temperature of HF-fed mice was significantly lower than that of mice fed a LF diet (23.7 *versus* 25.4 °C; Fig. 1*G*). In parallel, heat release after 60 min of cold exposure was noticeably higher in LF-fed mice than in HF-fed mice as captured by thermal IR camera (Fig. 1*H*). The chronic cold exposure was associated with a significant reduction of core body temperature compared with mice kept at the ambient temperature (31.2 °C); this was more evident in mice in HF-diet mice *versus* LF-diet mice (28.43 *versus* 29.7 °C) (Fig. 1*I*). Furthermore, heat release was significantly lower in mice on HF diet compared with LF diet (Fig. 1*J*). To distinguish the thermogenic activation between classical brown fat and beige fat, iBAT and subcutaneous white adipose tissue (sWAT) from the inguinal area were collected. The UCP1 expression was significantly increased in response to cold exposure in LF-fed mice in both iBAT and sWAT. However, UCP1 levels remained unchanged in HF-fed mice (Fig. 1, *K* and *L*), implicating an impairment of adaptive thermogenesis with chronic activation of TLR4 by HF diet. Supporting these results, H&E staining revealed that adipocyte size of iBAT was bigger in HF-fed mice than LF-fed mice at 25 °C, which remained unchanged after cold exposure to 8 °C. In contrast, iBAT from LF-fed mice became significantly smaller, implicating BAT activation (Fig. 1*M*). Similarly, adipocyte size of sWAT was significantly smaller in LF-fed mice than HF-fed mice at 25 °C. More importantly, brown-like adipocyte morphology was absent in HF-fed mice upon cold treatment (Fig. 1*N*).

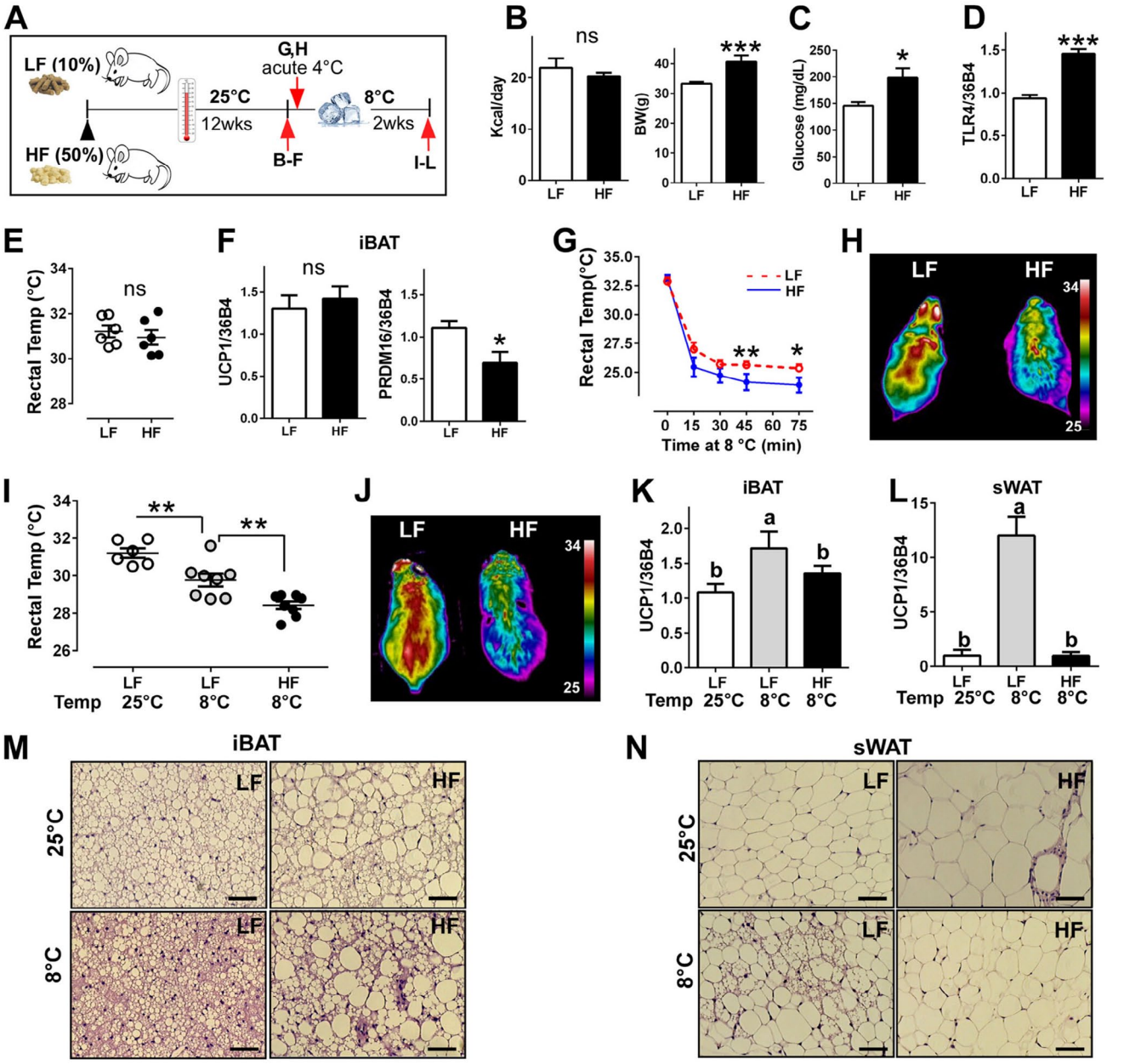

Figure 1. HF diet-induced TLR4 activation impaired adaptive thermogenesis — ***A,*** experimental scheme to determine the impacts of HF diet on adaptive thermogenesis. ***B–F,*** C57BL/6 mice were fed with HF *versus* LF diet for 12 weeks at 25 °C (n = 8 per group). ***B,*** total calorie intake per day (*left*) and body weight difference (*right*). *ns*, not significant. ***C,*** fasting glucose levels. ***D,*** TLR4 mRNA expression by qPCR at the end of 12 weeks of the diet. ***E,*** core body temperature by rectal thermometer at the end of 12 weeks of diet. ***F,*** gene expression of UCP1 and PRDM16 by qPCR of iBAT. ***G*** and ***H,*** C57BL/6 mice were fed with the LF or HF diet for 12 weeks at 25 °C and exposed to 8 °C acutely. ***G,*** core body temperature upon cold exposure for 75 min (n = 6 per group); *red* = LPS–, *blue* = LPS+. ***H,*** representative thermography captured by an IR camera (n = 6–8). ***I–N,*** C57BL/6 mice were fed with HF *versus* LF diet for 12 weeks at 25 °C, then transferred to 8 °C for an additional 2 weeks (n = 8 per group). ***I,*** core body temperature upon cold acclimation. ***J,*** representative thermography captured by an IR camera upon cold acclimation. ***K,*** UCP1 gene expression of iBAT after cold acclimation. ***L,*** UCP1 gene expression of sWAT after cold acclimation. ***M,*** representative images of H&E staining from iBAT (*scale bar* = 100 μm). ***N,*** representative images of H&E staining from sWAT (*scale bar* = 100 μm). All data are presented as the mean ± S.E.
* $p < 0.05$; ** $p < 0.01$; *** $p < 0.001$ by Student's t test. Values not sharing a common letter differ significantly ($p < 0.05$) by one-way ANOVA.

TLR4 Activation by LPS Inhibited Adaptive Thermogenesis— It has been established that LPS-mediated metabolic endotoxemia is associated with obesity and insulin resistance (26). However, its impact on adaptive thermogenesis is unknown. To address this issue, TLR4 was activated by low-dose LPS administration in two temperature settings, 25 °C and 8 °C (Fig. 2*A*). LPS-injected animals at ambient temperature had a significant reduction in body weight and adipose tissue mass compared with saline-injected mice (Fig. 2, *B* and *C*), presumably due to an inflammation-mediated lipolysis. Reflecting the augmented lipolysis in LPS injected mice, H&E staining revealed that subcutaneous fat exhibited smaller adipocytes and higher macrophage infiltration compared with the saline control. Additionally notable, lipid droplets of iBAT were smaller in LPS-injected mice, implicating

augmented lipolysis with LPS (Fig. 2*D*). We also confirmed that LPS administration increased fasting plasma glucose (Fig. 2*E*) but decreased adiponectin levels (Fig. 2*F*). Despite the manifested metabolic dysfunction, there was no significant difference in core body temperature at 25 °C (Fig. 2*G*). Upon acute cold exposure, LPS-injected mice displayed significantly lower core body temperatures (Fig. 2*H*) and decreased heat release (Fig. 2*I*) compared with saline controls. That was similar to the defective thermogenesis in chronic HF diet (Fig. 1, *G* and *H*). Chronic exposure to 8 °C for 2 weeks caused a significant increase in food intake and

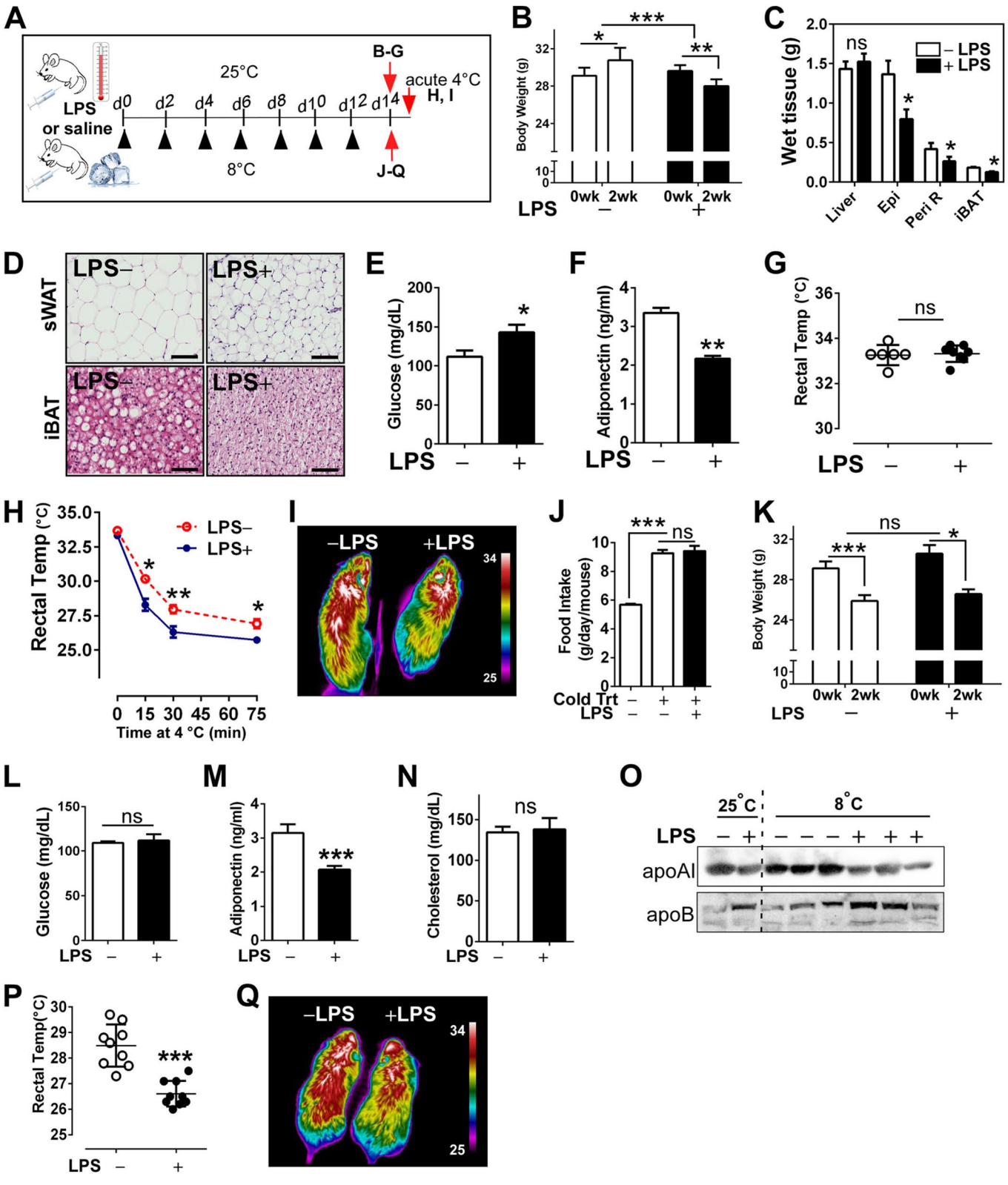

weight loss regardless of LPS administration (Fig. 2, *J* and *K*). Cold acclimation reversed the LPS-induced hyperglycemia (Fig. 2*L*) but not adiponectin levels (Fig. 2*M*). Although there was no difference in total cholesterol levels (Fig. 2*N*), LPS stimulation caused a reciprocal increase of apoB *versus* apoAI, which was worsened by cold acclimation (Fig. 2*O*). Moreover, LPS injection was associated with lower core body temperature (Fig. 2*P*) as well as reduced heat release (Fig. 2*Q*) *versus* saline control.

In summary, TLR4 activation by administration of a low dose of LPS 1) promotes metabolic dysfunction in glucose and lipid metabolism and 2) impedes the thermogenic potential for adapting to both acute and chronic cold exposure.

TLR4 Activation by LPS Attenuates Browning of sWAT— Next, we hypothesized that compromised thermogenesis in TLR4 activation is due to defective browning. First of all, TLR4 activation of sWAT samples was determined by qPCR. Chronic low-grade LPS injection significantly increased TLR4 mRNA expression compared with saline control (Fig. 3*A*, *left*). The gross images of sWAT collected from both axillary and inguinal areas of cold-acclimated mice showed the distinct dark brownish color implying the development of beige adipocytes. In contrast, LPS-injection was associated with diminished brownish color compared with saline injection (Fig. 3*A*, *right*). In parallel, brown-like adipocyte morphology was absent in LPS-injected mice despite the cold treatment (Fig. 3*B*). LPS stimulation dampened UCP1 protein levels as well as mitochondrial-specific protein expressions including VDAC, PDH, and cytochrome *c* (*Cytc*), the mitochondrial proteins residing in outer membrane, matrix, and inner membrane of mitochondria, respectively (Fig. 3*C*). Accordingly, cold-induced brown-specific signature gene expressions of UCP1, PRDM16, PGC1α, and CIDEA were abolished in LPS-injected subcutaneous fat (Fig. 3*D*). The increase of mtDNA contents in cold-acclimated sWAT was dampened in LPS-injected mice (Fig. 3*E*). Collectively, these data indicate that TLR4 activation by LPS mitigates cold-induced sWAT browning and mitochondrial biogenesis.

TLR4 Activation by LPS Marginally Down-regulates iBAT Brownness but Worsens Epididymal WAT Inflammation—We further investigated whether LPS imposes adverse impacts on classical brown fat and epididymal fat upon cold exposure. There was no significant change in iBAT mass (Fig. 3*F*). iBAT from LPS-injected mice appeared lighter in its distinct brown color (Fig. 3*G*) and seemingly contained more lipid than those from the saline controls (Fig. 3*H*). There was a slight decrease of UCP1, VDAC, and PDH in LPS-injected iBAT (Fig. 3*I*) despite that magnitudes of down-regulation were lesser than those found in sWAT (Fig. 3*C*). In contrast to sWAT (Fig. 3, *A*–*E*), cold exposure had a marginal impact on UCP1 gene expression and mtDNA contents in iBAT in both saline and LPS-injected groups (Fig. 3, *J* and *K*). On the other hand, cold exposure in the presence of LPS was associated with larger lipid droplets and augmented macrophage infiltration in epididymal fat (Fig. 3*L*). Consistently, the LPS-induced pro-inflammatory gene expression levels of IL-1β,TNFα, and F4/80 were increased along with the cold treatment (Fig. 3*M*).

TLR4 Activation-mediated Defective Browning Is Associated with ER Stress and Autophagic Activation—ER stress in adipose tissue links TLR4 activation to insulin resistance (19). We now raised the question of whether ER stress will be the primary pathway to suppress thermogenesis and WAT browning in TLR4 stimulation. Even in an ambient temperature setting, HF diet (Fig. 4*A*) or LPS administration (Fig. 4*B*) slightly increased the markers of ER stress such as CHOP, GRP78/BiP (ER chaperone), and JNK phosphorylation. Interestingly, ER stress markers were remarkably increased with cold exposure (Fig. 4, *A* and *B*). In accordance with the diminished UCP1 expression, phosphorylation of cAMP response element-binding protein (p-CREB) was reduced in LPS-injected subQ compared with saline controls. At ambient temperature there were no clear hints of autophagic activation in sWAT. However, TLR4 activation at 8 °C clearly increased the markers of autophagy such as LC3II, Beclin1, and Atg5 (Fig. 4, *A* and *B*). These data imply that autophagic degradation and ER stress are involved in TLR4-mediated defective thermogenesis.

LPS Attenuates cAMP-induced Browning in Human Adipocytes—To further determine the direct role of TLR4 activation in white adipocyte browning, we used an *in vitro* system. Primary cultures of human adipocytes derived from subcutaneous fat were treated with Bt_2cAMP, an analog of cAMP, in the presence or absence of LPS. The incubation of mature human adipocytes with Bt_2cAMP correlated with 1) induction of UCP1 and PGC1α gene expression (Fig. 5*A*), 2) increased oxygen consumption rate (Fig. 5*B*), and 3) mitochondrial biogenesis, evidenced by a rise in mtDNA contents (Fig. 5*C*) and Mito- Tracker red fluorescence (Fig. 5*D*). These effects were diminished almost to basal levels with the LPS pretreatment (Fig. 5, *A*–*D*), recapitulating the inhibitory effects of TLR4 activation on WAT browning *in vivo* (Figs. 1–3).

Subsequently, we attempted to determine the impact of LPS-triggered ER stress and autophagy activation on UCP1 expression and mitochondrial biogenesis. Consistent with an increase in mtDNA (Fig. 5*C*), Bt_2cAMP treatment alone caused VDAC induction (mitochondria-specific marker) and a slight induction of CHOP (ER stress marker). As we expected, LPS pretreatment nullified the cAMP-induced VDAC induction and increased CHOP activation. The suppression of lysosomal degradation by chloroquine accumulated LC3II with the double insult of cAMP and

Figure 2. LPS-induced TLR4 activation impaired adaptive thermogenesis. ***A,*** experimental scheme to determine the impacts of LPS administration on adaptive thermogenesis. ***B–G,*** low-dose LPS (LPS+) or saline (LPS–) was administered to C57BL/6 mice every other day (OE) for 2 weeks at 25 ºC (n = 8 per group). ***B,*** changes in body weight. ***C,*** wet tissue weight of liver, epididymal fat (*Epi*), peri-renal fat (*Peri R*), and iBAT. *ns*, not significant. ***D,*** representative microscopic images of sWAT and iBAT revealed by H&E staining (*scale bar* = 100 μm). ***E,*** fasting glucose level. ***F,*** adiponectin levels. ***G,*** core body temperature measured by rectal thermometer. ***H*** and ***I,*** after 2 weeks of either LPS or saline injection at 25 ºC, mice were acutely exposed to 8 ºC. ***H,*** core body temperature upon acute cold exposure for 75 min (n = 6 per group). ***I,*** representative thermography by IR camera. ***J–Q,*** low-dose LPS (LPS+) or saline (LPS–) was administered to C57BL/6 mice every other day for 2 weeks at 8 ºC (n = 8 per group). ***J,*** food intake at 8 ºC. ***K,*** body weight changes at 8 ºC. ***L,*** fasting glucose levels. ***M,*** plasma adiponectin levels. ***N,*** total cholesterol levels in plasma. ***O,*** plasma levels of apoB and apoAI. ***P,*** core body temperature of cold-acclimated mice. ***Q,*** representative thermography captured by IR camera after cold acclimation. All data are presented as the mean ± S.E. * $p < 0.05$; ** $p < 0.01$; *** $p < 0.001$ by Student's t test.

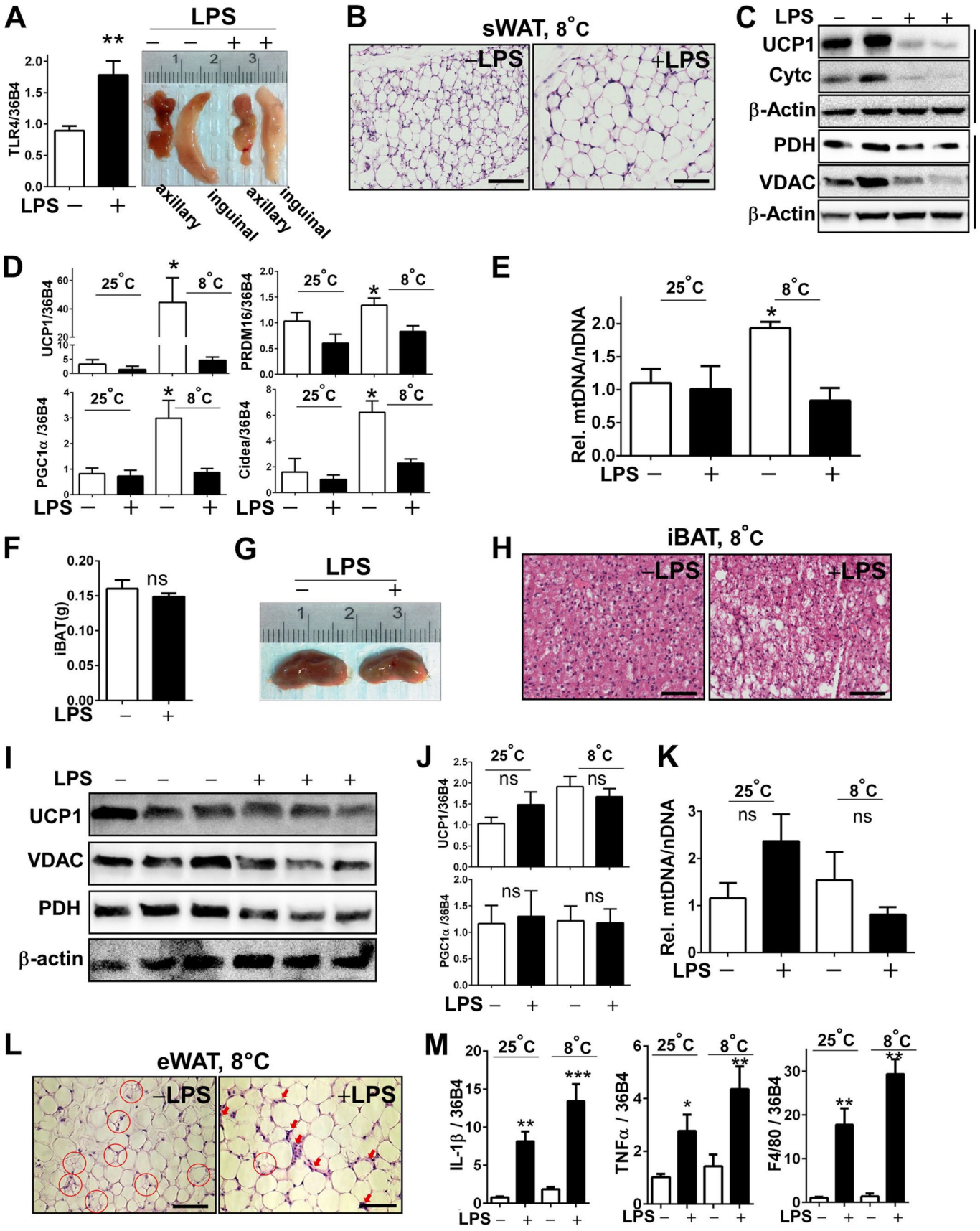
A
LPS
TLR4/36B4
axillary
inguinal
axillary
inguinal
B
sWAT, 8°C
–LPS
+LPS
C
LPS
UCP1
Cytc
β-Actin
PDH
VDAC
β-Actin
D
UCP1/36B4
PRDM16/36B4
PGC1α /36B4
Cidea/36B4
25°C
8°C
E
Rel. mtDNA/nDNA
F
iBAT(g)
ns
G
LPS
H
iBAT, 8°C
–LPS
+LPS
I
LPS
UCP1
VDAC
PDH
β-actin
J
UCP1/36B4
PGC1α /36B4
ns
K
Rel. mtDNA/nDNA
L
eWAT, 8°C
–LPS
+LPS
M
IL-1β / 36B4
TNFα / 36B4
F4/80 / 36B4

LPS, suggesting an increase of autophagic flux (Fig. 5*E*). Generation of ROS was significantly higher in LPS-stimulated adipocytes, which was comparable to ROS production in *t*-butyl hydroperoxide (*t-Bu-PO*) treatment, a positive control (Fig. 5*F*, *left*). The preloading of Mito TEMPO, a mitochondria-specific antioxidant, decreased ROS production to the basal levels (Fig. 5*F*, *right*), suggesting that mitochondria is the primary source of ROS production upon combinatory stimulation of LPS and cAMP adipocyte.

To determine the direct impact of ER stress on WAT browning, Tg, an ER stress inducer, was added to human adipocytes. Tg-induced ER stress completely abolished UCP1 gene expression (Fig. 5*G*). Similar to TLR4 activation by LPS stimulation, Tg stimulation reduced VDAC expression and increased autophagic flux (Fig. 5*H*). Next, CHOP was silenced using *si*RNA in primary human adipocytes. *si*CHOP caused an ~80% decrease of CHOP mRNA expression (Fig. 5*I*). Silencing of CHOP partly restored cAMP-inducible UCP1 expression upon LPS stimulation (Fig. 5*J*).

Collectively, these data suggest that TLR4 activation inhibits cAMP-inducible browning in primary human adipocytes, probably through mechanisms including mitochondria-driven ROS production, ER stress, and aberrant autophagic activation, which may synergistically lead to defective mitochondrial biogenesis.

Inhibition of ER Stress Conferred a Resistance against TLR4 Activation-induced Down-regulation of WAT Browning—We have shown that ER stress alone was sufficient to diminish UCP1 induction and causes mitochondrial dysfunction (Fig. 5*H*). Next, we conceived the question of whether ER stress is a necessary mechanism to inhibit WAT browning and thermogenesis in TLR4 activation. To address this we first prepared primary adipocytes derived from EMSC of either CHOP-deleted ($CHOP^{-/-}$) or wild-type mice ($CHOP^{+/+}$). The homozygous CHOP knock-out mice had virtually no mRNA and protein expression of CHOP (Fig. 6*A*). Surprisingly, adipocytes from $CHOP^{-/-}$ were resistant to the LPS-mediated down-regulation of UCP1 gene (Fig. 6*B*). The LPS-stimulated ROS production from the $CHOP^{-/-}$ adipocytes was not statistically significant from ROS production in adipocytes without LPS treatment (Fig. 6*C*).

There was no difference in core body temperature in cold-acclimated $CHOP^{-/-}$ mice between groups that received LPS or saline (Fig. 6*D*). Subsequently, we analyzed the sWAT to determine the effects of CHOP deletion on WAT browning. The mitochondrial DNA contents (Fig. 6*E*) as well as UCP1 and PGC1α gene expression levels (Fig. 6*F*) in cold-acclimated sWAT were identical regardless of LPS injection. In contrast to the results from cold-acclimated $CHOP^{+/+}$ mice (Fig. 4), LPS administration of $CHOP^{-/-}$ mice failed to down-regulate UCP1 and VDAC protein expression. In fact, VDAC expression was apparently higher in LPS-administered mice than in saline controls. LPS stimulation did not trigger LC3II accumulation or Atg5 induction (Fig. 6*G*), implicating that LPS-mediated aberrant autophagy under cold exposure is associated with the ER stress/CHOP pathway.

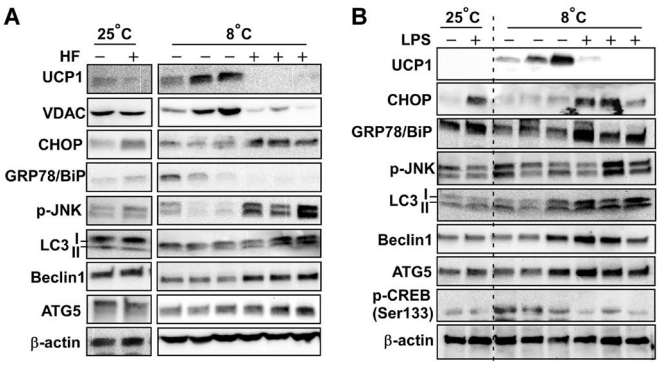

Figure 4. TLR4-mediated defective WAT browning was associated with ER stress and aberrant autophagy activation. ***A,*** mice were fed either with low fat (HF–) or high fat (HF+) in ambient (25 °C) or cold (8 °C) temperature (also see the scheme in Fig. 1*A*). sWAT were used for Western blot analysis for markers of WAT browning (UCP1, pCREB), ER stress (p-JNK, CHOP, BiP), and autophagy (LC3 I/II, Atg5, Beclin1). β-Actin used for loading control. ***B,*** mice were administered with either saline (LPS–) or low-dose LPS (LPS+) in ambient (25 °C) or cold (8 °C) temperature (also see the scheme in Fig. 2*A*). sWAT were used for Western blot analysis for makers of WAT browning, ER stress, and autophagy. Each band represents individual animal. Images are representative for two separate runs. *GPR78/Bip*, G-protein-coupled receptor 78 (also referred to as BiP); *p-CREB*, phosphorylated-cAMP response element binding protein (Ser-133).

To further confirm the role of ER stress in WAT browning, C57BL/6 mice were administered with PBA, a chemical chaperone that inhibits ER stress (27), along with LPS for 2 weeks at 8 °C. Similar to the mice devoid of CHOP, mice co-administered with LPS and PBA managed to keep their body temperature higher than mice administered with LPS alone (Fig. 6*H*). The co-administration with PBA prevented LPS-mediated CHOP activation in sWAT (Fig. 6*I*). Consistent with $CHOP^{-/-}$ mice, inhibition of ER stress by PBA restored UCP1 and VDAC expression but reduced beclin1 and LC3II accumulation as opposed to LPS stimulation alone (Fig. 6*I*). These data suggest that inhibition of ER stress either by genetic deletion of CHOP or chemical inhibition by PBA confers resistance to the TLR4-mediated down-regulation of sWAT browning and thermogenesis.

TLR4 Deletion Protected against LPS-induced Down-regulation of WAT Browning and Thermogenesis—The deletion of metabolically active TLR4 has been shown to attenuate LPS-mediated ER stress (19). Lastly, we investigated whether the deletion of TLR4 reverses the LPS-mediated WAT browning and thermogenesis.

☜ **Figure 3.** LPS administration inhibited cold acclimation-induced WAT browning and mitochondrial biogenesis. C57BL/6 mice received either saline or LPS injection every other day for 2 weeks at 8 °C. ***A,*** TLR4 mRNA expression by qPCR (*left*) and gross images of axillary and inguinal adipose tissue after cold acclimation (*right*). ***B,*** representative microscopic images of sWAT revealed by H&E staining (*scale bar* = 100 μm). ***C,*** immunoblot analysis of sWAT for UCP1, VDAC, PDH, and cytochrome *c* (*Cytc*). ***D,*** relative gene expression levels of brown-specific markers of UCP1, PRDM16, PGC1α, and CIDEA in sWAT measured by qPCR. ***E,*** relative mtDNA contents normalized by nuclear DNA in sWAT. ***F,*** tissue mass of iBAT. *ns*, not significant. ***G,*** representative gross image of iBAT after cold acclimation. ***H,*** representative microscopic images of iBAT revealed by H&E staining (*scale bar* = 100 μm). ***I,*** immunoblot analysis of iBAT for UCP1, VDAC, and PDH. ***J,*** relative gene expression levels of UCP1 and PGC1α in iBAT by qPCR. ***K,*** relative mtDNA contents in iBAT. ***L,*** representative microscopic image of epididymal WAT (*eWAT*) after cold acclimation. Adipocytes undergoing lipolysis are marked in *red circles*. Macrophage infiltration is marked in *red arrows* (*scale bar* = 100 μm). ***M,*** relative gene expression of IL-1β, TNFα, and F4/80 in epididymal WAT. All data are presented as the mean ±S.E. * $p < 0.05$; ** $p < 0.01$; *** $p < 0.001$ by Student's *t* test.

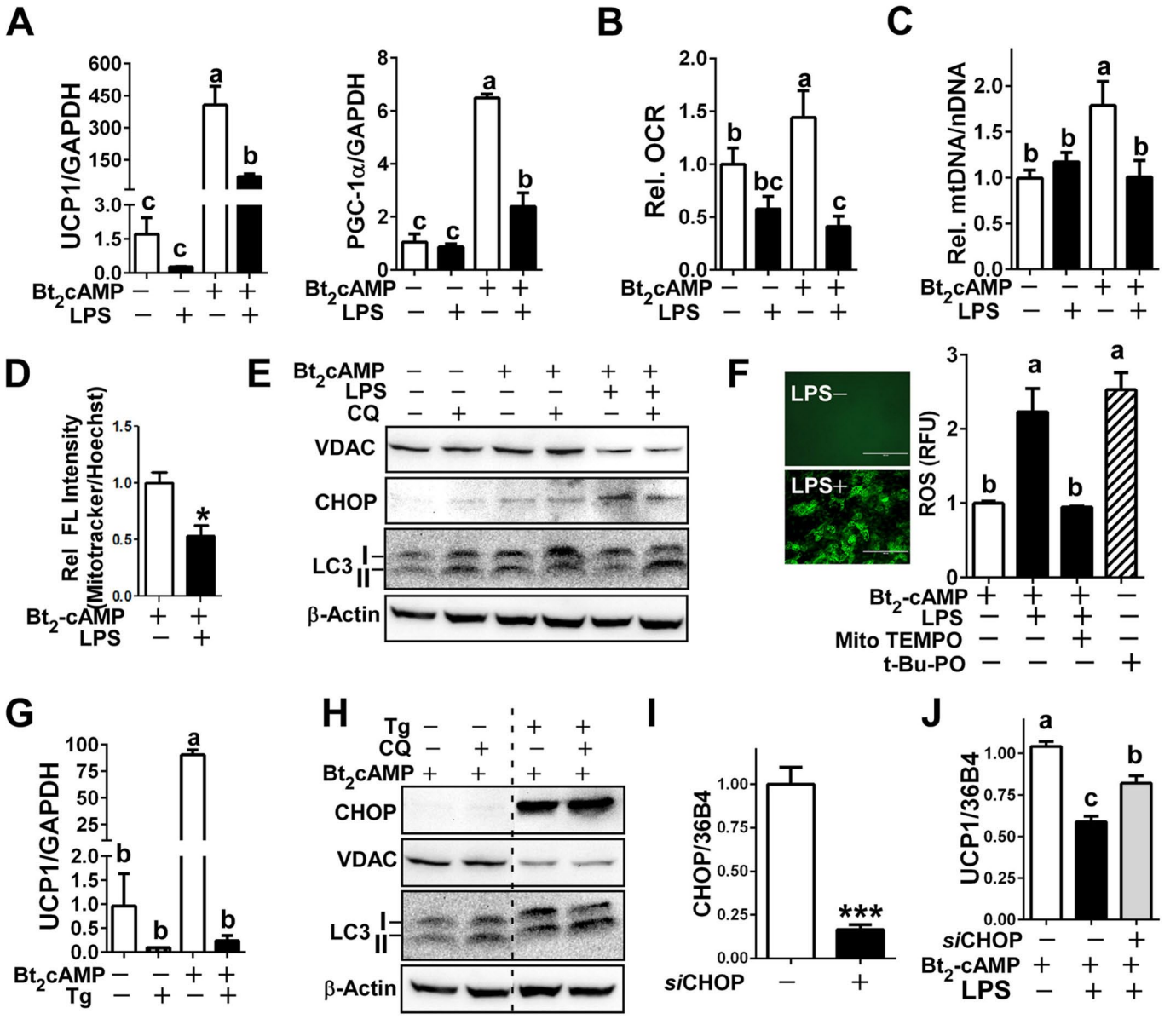

Figure 5. LPS attenuated cAMP-induced browning in primary human adipocytes. ***A–F,*** primary cultures of human adipocytes were pretreated with or without LPS (100 ng/ml) for 72 h followed by Bt_2cAMP (0.5 mM) stimulation for 6–12 h (n = 4/group with duplication). ***A,*** relative gene expression of UCP1 and PGC1α by qPCR. ***B,*** oxygen consumption rate (*OCR*). ***C,*** relative mtDNA contents. ***D,*** relative abundance of mitochondria by MitoTracker florescence normalized by nucleus Hoechst staining. ***E,*** immunoblot analysis of VDAC, LC3, CHOP, and β-actin. Chloroquine (*CQ*) was added at the last 3 h of total 6 h of Bt_2cAMP stimulation. ***F,*** *in situ* ROS production captured by fluorescence microscopy (*left*), ROS production in the presence (+) or absence (–) of LPS and Mito-TEMPO (*right*). *t*-Butyl hydroperoxide (*t*-Bt-PO) was used as a positive control for ROS production. ***G*** and ***H,*** mature human adipocytes were preincubated with Tg for 12 h followed by Bt_2cAMP stimulation for 12 h (n = 4/group with duplication). ***G,*** relative UCP1 mRNA expression in the presence of Tg stimulation. ***H,*** immunoblot analysis of CHOP, VDAC, and LC3 I/II. Chloroquine was added at the last 3 h of Bt_2cAMP stimulation. ***I*** and ***J,*** human mature adipocytes were either transfected with *si*CHOP (*siCHOP*+) or non-targeting *si*Cont (*siCHOP*–). ***I,*** mRNA expression of CHOP after 72 h of transfection. ***J,*** relative UCP1 mRNA expression in CHOP silenced human adipocytes. All data are presented as the mean ± S.E. * $p < 0.05$ by Student's t test. Values not sharing a common letter differ significantly by one-way ANOVA.

$TLR4^{-/-}$ adipocytes were prepared from EMSC of the homozygous $TLR4^{-/-}$ mice. In $TLR4^{-/-}$ adipocytes (Fig. 7*A*), cAMP-mediated UCP1 mRNA expressions were not statistically different between LPS *versus* saline treatment (Fig. 7*B*). Also, the decrease of mitochondrial DNA contents in response to LPS and cAMP in wild-type ($TLR4^{+/+}$) adipocytes was restored in $TLR4^{-/-}$ adipocytes (Fig. 7*C*). Similarly, LPS-induced down-regulation of VDAC and CREB phosphorylation was restored in $TLR4^{-/-}$. Unexpectedly, autophagy levels were higher in $TLR4^{-/-}$ (Fig. 7*D*), which is seemingly a separate mechanism rather than a consequence of ER stress-mediated mitochondrial degradation.

Next, $TLR4^{-/-}$ mice were transferred to 8 °C and administered with either saline or LPS for 2 weeks. There was no difference in core body temperature (Fig. 7*E*) or IR thermography (Fig. 7*F*). The gene expression levels of UCP1 and PGC1α in sWAT were not different irrespective of LPS administration (Fig. 7*G*). LPS-inducible

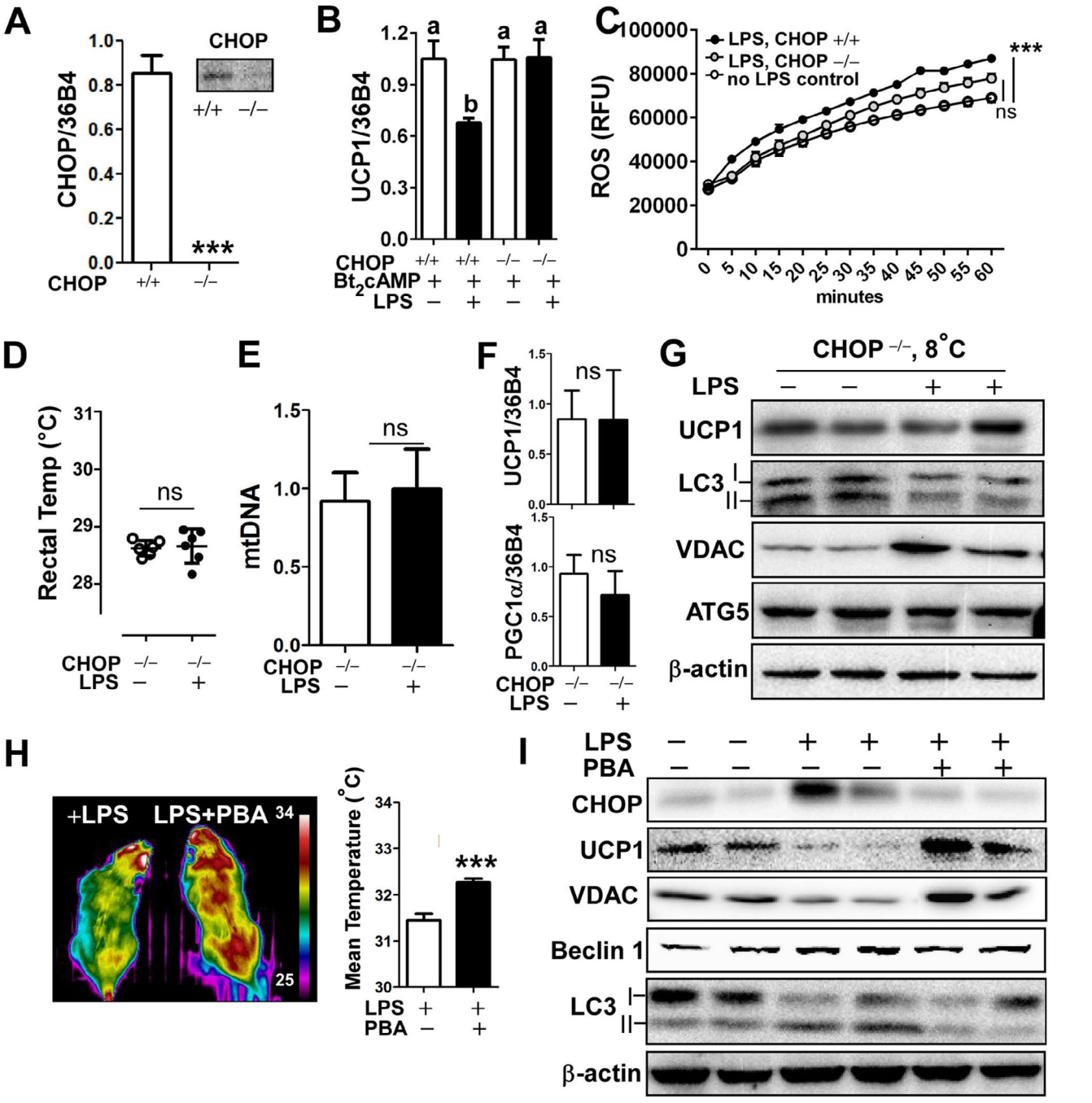

Figure 6. Inhibition of ER stress attenuated LPS-induced down-regulation of WAT browning and adaptive thermogenesis. ***A–C,*** primary adipocytes were prepared from EMSC of wild-type (*CHOP*$^{+/+}$) and CHOP deleted (*CHOP*$^{-/-}$) mice (n = 4/group). ***A,*** relative expression of mRNA of CHOP in CHOP$^{+/+}$ *versus* CHOP$^{-/-}$ adipocytes. ***B,*** relative expression of UCP1 with or without LPS pretreatment for 72 h followed by Bt_2cAMP stimulation for 6 h. ***C,*** LPS-inducible ROS production in CHOP$^{+/+}$ *versus* CHOP$^{-/-}$ adipocytes (n = 12). *RFU*, relative fluorescence units. *** $p < 0.001$ by two-way ANOVA with repeated measure. ***D–G,*** CHOP$^{-/-}$ mice received either saline or LPS injection every other day for 2 weeks at 8 ºC (n = 6 per group). ***D,*** core body temperature measured by rectal thermometer. ***E,*** mtDNA contents in sWAT after cold-acclimation. ***F,*** relative expression of UCP1 and PGC1α by qPCR of sWAT. ***G,*** Western blot analysis of UCP1, LC3I/II, VDAC, Atg5, and β-actin. ***H*** and ***I,*** C57BL/6 mice were injected with either saline, LPS alone, or LPS plus PBA (200 mg/kg/day) for 2 weeks at 8 ºC (n = 7 per each group). ***H,*** representative thermography captured by IR camera after cold acclimation (*left*). Mean surface body temperature was analyzed (*right*). ***I,*** Western blot analysis of CHOP, UCP1, LC3I/II, VDAC, Beclin1, and β-actin. All data are presented as the mean ± S.E. *** $p < 0.001$ by Student's t test; *ns*, non-significant. Values not sharing a common letter differ significantly ($p < 0.05$) by one-way ANOVA.

CHOP activation was markedly reduced in sWAT of TLR4$^{-/-}$ compared with TLR4$^{+/+}$ (Fig. 7*H*). Consistently, LPS-mediated down-regulation of UCP1 protein expression and mitochondrial proteins of VADC and cytochrome *c* were restored to comparable levels found in saline control (Fig. 7*H*). Similar to the cell study (Fig. 7*D*), TLR4 deletion itself had higher levels of LC3II expression,

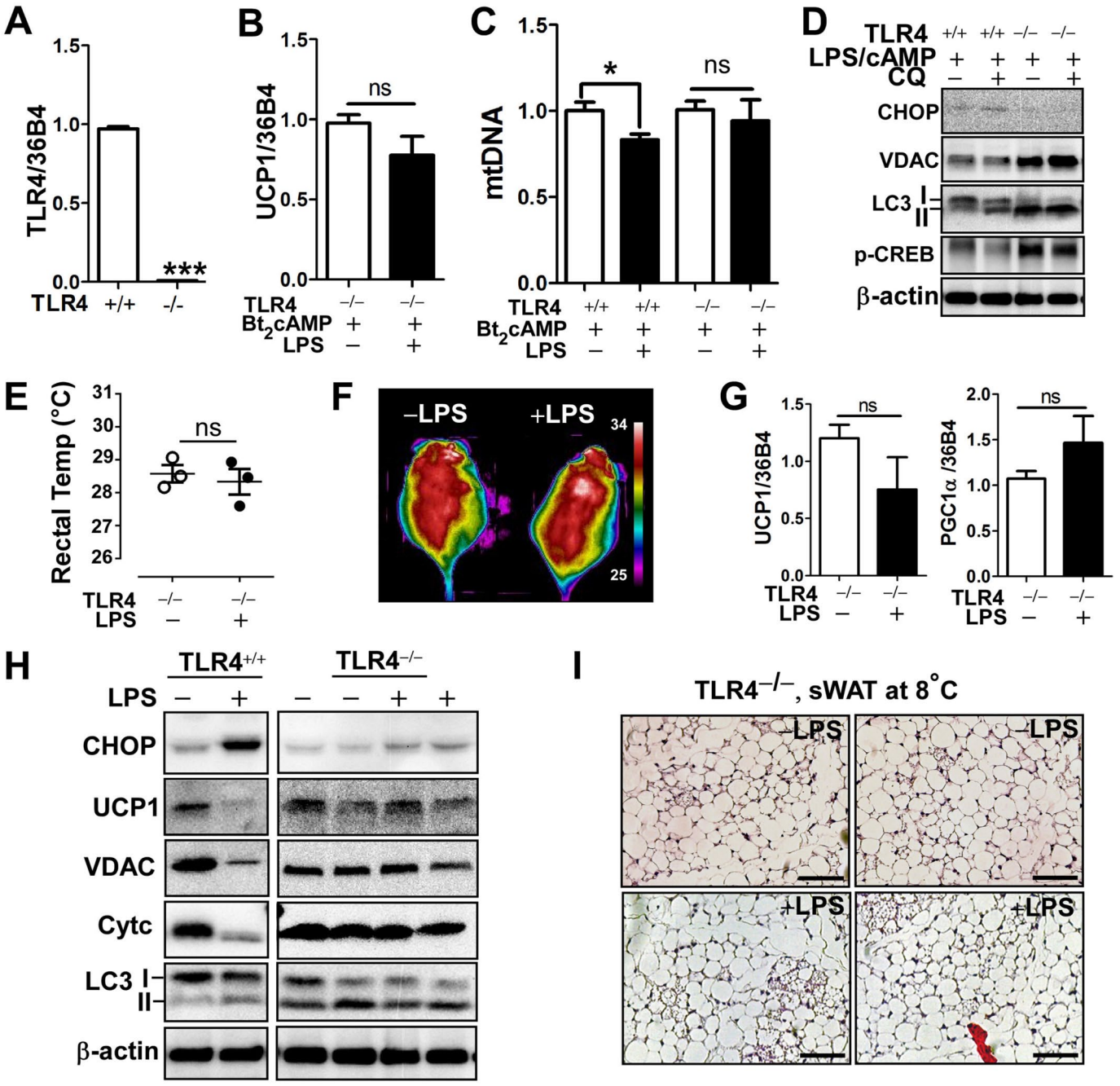

Figure 7. Deletion of TLR4 protected from LPS-induced attenuation of WAT browning and thermogenesis**. *A–D,*** primary adipocyte cultures were prepared from EMSC of wild-type (*TLR*$^{+/+}$) and TLR4 deleted (*TLR4*$^{-/-}$) mice. ***A,*** relative mRNA expression of TLR4. ***B,*** relative expression of UCP1 with or without LPS pretreatment for 72 h followed by Bt_2cAMP stimulation for 6 h. ***C,*** mtDNA contents. ***D,*** Western blot analysis of CHOP, LC3I/II, VDAC, cAMP response element-binding protein (*p-CREB*), and β-actin. ***E–J,*** TLR4$^{-/-}$ mice received either saline or LPS injection every other day for 2 weeks at 8 °C (n = 4–5 per group ***E.*** Core body temperature measured by rectal thermometer. ***F,*** representative thermography captured by IR camera after cold acclimation. ***G,*** relative mRNA expression of UCP1 and PGC1α of sWAT. ***H,*** Western blot analysis of CHOP, UCP1, LC3I/II, VDAC, cytochrome *c* (*Cytc*) and β-actin. ***I,*** H&E staining from sWAT of TLR4$^{-/-}$ mice injected with LPS or saline (*scale bar* = 100 μm). All data are presented as the mean ± S.E. * $p < 0.05$; *** $p < 0.001$ by Student's t test; *ns*, non-significant.

which did seem to cause mitochondrial degradation (Fig. 7*H*). The morphological changes in TLR4-deleted adipose tissue was also investigated by H&E. Unlike the LPS-injected wild-type mice (TLR4$^{+/+}$) at 8 °C (Fig. 3*B*), there was no significant difference of adipocyte size and appearance of brown-like adipocytes between LPS and saline-injected TLR4$^{-/-}$ mice (Fig. 7*I*). Together, these data showed that TLR4 activation is a crucial contributor to ER stress activation and subsequent modification for browning and thermogenesis in sWAT.

Discussion

Obesity is defined as a chronic low-grade inflammatory status (meta-inflammation) wherein mitochondrial function is frequently compromised (28). Few observations have been made to

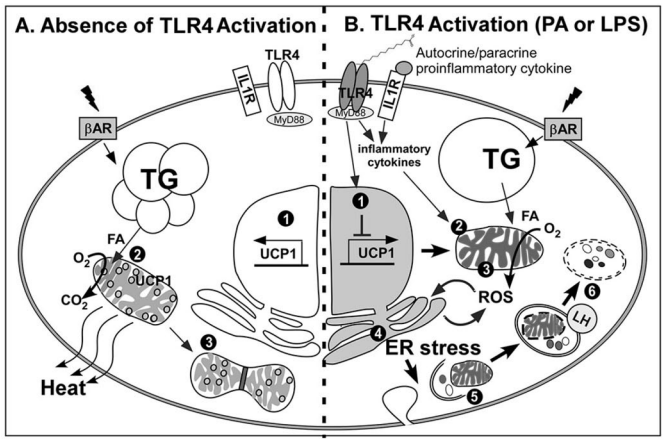

Figure 8. The working model that TLR4 activation represses WAT browning and adaptive thermogenesis. ***A,*** in the absence of TLR4 activation, β-adrenergic receptor (β-*AR*) signaling stimulates 1) transcriptional activation of UCP1, 2) UCP1-mediated heat release upon free fatty acid influx into healthy mitochondria, and 3) mitochondrial biogenesis. ***B,*** TLR4 activation by either HF diet or LPS triggers: 1) TLR4-mediated inflammatory signaling that counteracts UCP1 expression and secretes proinflammatory cytokines; 2) autocrine/ paracrine action of inflammation, which causes mitochondrial dysfunction; 3) inflamed mitochondria, which induces incomplete oxidative phosphorylation resulting in production of ROS; 4) ROS production from mitochondria, which causes ER stress; 5) ER stress activation, which initiates aberrant autophagy; 6) defective organelles including mitochondria, which are removed by lysosomal degradation. As a consequence of TLR4 activation, sWAT becomes immune to the signaling cues for thermogenic activation. *LH*, lysosomal hydrolase; *TG*, triglyceride; *FA*, fatty acid.

determine the metabolic consequences of inflamed white adipocyte upon browning signal. The goal of this study was to identify the molecular mechanisms underlying the defective WAT browning and adaptive thermogenesis in obesity. Here we demonstrated that TLR4 activation impaired cold-induced WAT browning and thermogenic activation (Figs. 1 and 2). TLR4-mediated ER stress was associated with ROS production, aberrant autophagy, and reduced mitochondrial content upon cold treatment (Figs. 4 and 5). Inactivation of ER stress by either genetic deletion of CHOP or chemical ER chaperone prevented TLR4-mediated autophagic activation and restored mitochondrial content (Fig. 6). Moreover, ablation of TLR4 conferred a resistance to LPS-induced ER stress in sWAT, reverting thermogenesis potential to normal (Fig. 7). Based on these results, here we propose a model that TLR4/ER axis activation promotes mitochondrial loss hindering WAT browning and adaptive thermogenesis (Fig. 8). To our knowledge this is the first study reporting TLR4 as a negative regulator of WAT browning and adaptive thermogenesis.

It is well characterized that TLR4 is a lipid sensor that could be activated by natural ligand palmitate (17) as well as endotoxin LPS (26). Our study started by asking, Does TLR4-mediated inflammation undermine WAT browning and adaptive thermogenesis? To answer this question, we compared the impact of TLR4 activation (either by palmitate or by LPS) on browning in different temperature settings (ambient *versus* cold). There were no detectable differences in mice core body temperatures in TLR4 activation at ambient environment (Figs. 1*E* and 2*G*). Upon acute cold exposure, however, TLR4 activation was associated with a noticeable decrease in maintaining temperature homeostasis (Figs. 1*G* and 2*H*), indicating that TLR4 activation attenuates acute thermogenic potential. Likewise, upon chronic cold exposure, TLR4 stimulation was associated with lower body temperature (Figs. 1*I* and 2*P*) absent of brown-like morphology in sWAT (Figs. 1*N* and 3*B*) and reduced thermogenesis (Figs. 1*J* and 2*Q*). With these results, we conclude that TLR4 activation is inversely associated with thermal adaptation upon chronic as well as acute cold exposure.

Down-regulation of BAT activity could be due to a plethora of reasons. A recent study from Bae *et al.* (29) reported that activation of pattern-recognition receptors such as NOD-like receptors (NLR) or toll-like receptors (TLR) inhibit peroxisome proliferator-activated receptor γ transactivation in brown (or beige) precursor cells, resulting in suppression of brown-specific marker genes. This notion aligns with our finding that LR4 activation repressed the transcriptional activation of beige-specific marker gene expression *in vivo* (Figs. 1, *K* and *L*, and 3*D*) as well as *in vitro* (Fig. 5*A*). These data suggest that stimulation of pattern-recognition receptors, at least TLR4, restrict the brown activation via transcriptional regulation.

Besides the transcriptional regulation (30), we focused on investigating the signaling events. ER stress activation has been recognized as a key signaling pathway linking TLR4-mediated adipose inflammation to obesity and insulin resistance. Although chronic-HF feeding has been shown to trigger ER stress and NF-κB activation in epididymal WAT (31), it has not been reported whether sWAT will also be susceptible to ER stress. Our results revealed that ER stress activation was significantly higher in TLR4-stimulated animals kept in cold than those housed at ambient temperature (Figs. 4, *A* and *B*). These results lead us to hypothesize that TLR4-mediated mitochondrial dysfunction will cause inappropriate handling of free fatty acid substrate through oxidative respiratory chain complexes, resulting in ROS production and ER stress in sWAT. This hypothesis is supported by our results showing that mitochondria are the primary source of ROS production (Fig. 5*F*). Also, Kawasaki *et al.* (31) reported that mitochondria-originated ROS induces ER stress upon the surge of free fatty acid influx in TNFα-primed 3T3L1 adipocytes. Intriguingly, ROS production by LPS is significantly reduced in $CHOP^{-/-}$ adipocytes compared with $CHOP^{+/+}$ adipocytes (Fig. 6*C*), suggesting a mutual ER-mitochondria interaction for ROS production.

Another important signaling pathway that we focused on was autophagic activation. Autophagy is the self-digestive recycling process that mediates lysosomal degradation of damaged or superfluous cellular components for adaptation to stress or survival (32). Inhibition of autophagy pathway abolishes white adipocyte differentiation and switches WAT to BAT *in vivo* (33, 34). In contrast, markers of autophagic activation (insoluble LC3II formation) are abnormally high in obesity (35–37). Also, pathological WAT from diabetic patients possess excessive autophagy activity (37). Therefore, it is plausible to think that inhibition of autophagy to secure the sufficient number of mitochondria might be a prerequisite for browning. Inversely, high levels of lysosomal degradation of mitochondria through autophagy will deter WAT from phenotypic switching to beige. Throughout the study, we consistently detected that ER stress was followed by aberrant autophagic activation in sWAT (Fig. 4), which was apparently associated with mitochondrial degradation or reduced mitochondrial biogenesis (Fig. 5, *C*–*E*). Based on the intimate relationship be-

tween ER stress and autophagy, we propose that TLR4-mediated ER stress in sWAT inhibits browning via autophagic degradation of mitochondria. Supporting this notion, deletion of CHOP protected LPS-mediated down-regulation of thermogenesis and mitochondrial loss (Fig. 6). These results also align with the study that CHOP deletion confers resistance to HF diet-mediated metabolic complications despite marked obesity (38).

Taken together we propose our working model by which TLR4 activation suppresses adaptive thermogenesis and browning. In this model we introduce a previously unappreciated signaling network connecting TLR4-mediated inflammation, mitochondrial dysfunction, ER stress, and autophagic degradation of mitochondria and thereby defective browning of sWAT (Fig. 8). Although it was logically built based on our data and literature support, our model still exhibits some missing links. One of the undefined links is between ER stress-induced autophagic activation and dynamic regulation of mitochondria. It needs to be defined whether ER stress triggers non-selective macroautophagy or mitophagy. Also, more evidence is required to set the role of TLR4 activation on mitochondrial biogenesis *versus* degradation.

The most responsive cells to ligand binding to TLR4 are macrophages. Adipose tissue macrophages are critical factors regulating adipose tissue quality depending on their polarization status. The macrophage polarization into proinflammatory M1 status causes obesity-mediated metabolic complications (39). Conversely, alternatively polarized M2 macrophages promote WAT browning (40). Recently, Sakamoto *et al.* (41) have reported that conditioned medium from LPS-stimulated RAW macrophages was able to decrease UCP1 induction in C3H10T1/2 adipocytes by decreasing the promoter activities of UCP1 and cAMP-response element (CRE). These data indicate that TLR4-mediated innate immune responses from macrophages exert potent paracrine action to attenuate WAT browning. Furthermore, TLR4 activation by a palmitate-rich diet can stimulate inflammasome formation in macrophages and subsequent release of IL-1β, one of most cytotoxic cytokines, impairing insulin sensitivity in adjacent adipocytes (42). Supporting these studies, our preliminary studies showed that IL1β-containing conditioned medium from murine macrophages effectively inhibited cAMP-mediated induction of UCP1 and PGC1α in primary murine adipocytes (data not shown). Even though TLR4 stimulation in adipocytes alone was sufficient to attenuate browning (Fig. 5*A*), it is likely that TLR4-mediated defective browning and thermogenesis *in vivo* could be the result of a synergistic interaction between macrophages and adipocytes. In an attempt to further confirm the critical role of TLR4 in WAT browning, we used $TLR4^{-/-}$ mice. It was not a surprise to see that $TLR4^{-/-}$ mice were resistant to LPS-mediated CHOP activation and down-regulation of browning (Fig. 7). It also lines up with the previous studies that TLR4 knockout or loss of function of TLR4 were resistant to HF diet-mediated ER stress, obesity, and insulin resistance (18–20).

Browning of WAT is the systemic response interplayed by multiple factors in systemic levels including hypothalamus, muscle, liver, and heart in addition to sWAT (1). Particularly, the central nervous system, *i.e.* hypothalamus, plays a key role in regulating food intake, body temperature, and energy expenditure. Central inflammation has been shown to cause obesity and metabolic dysfunction (43). Arruda *et al.* (44) have demonstrated that low-grade hypothalamic inflammation inversely regulates thermogenesis and insulin sensitivity. In the current study we did not investigate the impact of central inflammation by TLR4 on catecholamine levels, thermogenic hormones of orexin, or brain-derived neurotrophic factor. Likewise, we did not explore potential contributions from thermogenic endocrine factors such as myogenic hormone irisin or hepatic hormone FGF21. An increase of irisin secretion from muscle has been previously demonstrated both in humans and rodents during exercise and cold exposure (45). Therefore, it would be of interest to investigate whether TLR4 stimulation alters neural and endocrine regulators of WAT browning in future studies.

There is accumulating evidence that transplantation of a small amount of brown fat reverses or attenuates obesity and insulin resistance in recipient rodents (46, 47). In contrast to the immediate benefits corresponding to an increase of functional BAT mass or activity, therapeutic use of β-agonists or other sympathomimetics in humans was unsuccessful in enhancing browning or BAT activity (48, 49). Our study may provide a metabolic hint to explain the ineffectiveness of these pharmacological trials. The administration of β-agonist or thyroid hormones (or mimics) to the patients who have persistent meta-inflammation may not initiate the browning. The constitutively active ER stress and high autophagic flux in obesity will interfere with the singling cues for browning in its target tissue, sWAT. Therefore, we envision that prior or simultaneous administration of ER stress inhibitor along with β-agonists (or other sympathomimetics) would facilitate the white-to-beige conversion by dampening the inhibitory signaling pathways.

Here we present that TLR4/ER stress as a primary signaling axis suppressing adaptive thermogenesis and browning in obesity. Despite the fact that there are some missing links, our proposed model (Fig. 8) may pose a clinical significance by revealing the signaling cross-talk between TLR4-induced inflammation and adipocyte browning. Our study will provide a novel insight into the development of alternative therapeutic strategies to augment BAT activity. Clearly, the attenuation of pre-existing inflammation and ER stress in obesity should be addressed before therapeutic trials to boost BAT activity.

Author contributions — M. O. and S. C. conceived and coordinated the study and wrote the paper. M. O., W. W., and I. K. performed the experiments and analyzed the data. A. P. and T. C. performed GC analysis for FA profiles of diet and animal tissue. All authors reviewed the results and approved the final version of the manuscript.

Acknowledgments — This work was supported, in whole or in part, by National Institutes of Health Grant 1P20GM104320 (Project 5; to S. C.). We thank Guobin Kang for technical support in processing adipose tissue samples for histological analysis. We acknowledge Dr. Rolando Garcia (United States Department of Agriculture, North Dakota) for constructive discussion and Meri Nantz for reviewing the manuscript. The authors declare that they have no conflicts of interest with respect to the contents of this article.

References

1. Sidossis, L., and Kajimura, S. (2015) Brown and beige fat in humans: Thermogenic adipocytes that control energy and glucose homeostasis. *J. Clin. Invest.* 125, 478–486
2. Seale, P., Bjork, B., Yang, W., Kajimura, S., Chin, S., Kuang, S., Scimè, A., Devarakonda, S., Conroe, H. M., Erdjument-Bromage, H., Tempst, P., Rudnicki, M. A., Beier, D. R., and Spiegelman, B. M. (2008) PRDM16 controls a brown fat/skeletal muscle switch. *Nature* 454, 961–967
3. Rosenwald, M., and Wolfrum, C. (2014) The origin and definition of brite versus white and classical brown adipocytes. *Adipocyte* 3, 4–9
4. Giralt, M., and Villarroya, F. (2013) White, brown, beige/brite: Different adipose cells for different functions? *Endocrinology* 154, 2992–3000
5. Rosenwald, M., Perdikari, A., Rülicke, T., and Wolfrum, C. (2013) Bi-directional interconversion of brite and white adipocytes. *Nat. Cell Biol.* 15, 659–667
6. Lee, Y. K., and Cowan, C. A. (2013) White to brite adipocyte transition and back again. *Nat. Cell Biol.* 15, 568–569
7. Sharp, L. Z., Shinoda, K., Ohno, H., Scheel, D. W., Tomoda, E., Ruiz, L., Hu, H., Wang, L., Pavlova, Z., Gilsanz, V., and Kajimura, S. (2012) Human BAT possesses molecular signatures that resemble beige/brite cells. *PLoS One* 7, e49452
8. Wu, J., Boström, P., Sparks, L. M., Ye, L., Choi, J. H., Giang, A. H., Khandekar, M., Virtanen, K. A., Nuutila, P., Schaart, G., Huang, K., Tu, H., van Marken Lichtenbelt, W. D., Hoeks, J., Enerbäck, S., Schrauwen, P., and Spiegelman, B. M. (2012) Beige adipocytes are a distinct type of thermogenic fat cell in mouse and human. *Cell* 150, 366–376
9. Cypess, A. M., Lehman, S., Williams, G., Tal, I., Rodman, D., Goldfine, A. B., Kuo, F. C., Palmer, E. L., Tseng, Y. H., Doria, A., Kolodny, G. M., and Kahn, C. R. (2009) Identification and importance of brown adipose tissue in adult humans. *N. Engl. J. Med.* 360, 1509–1517
10. van Marken Lichtenbelt, W. D., Vanhommerig, J. W., Smulders, N. M., Drossaerts, J. M., Kemerink, G. J., Bouvy, N. D., Schrauwen, P., and Teule, G. J. (2009) Cold-activated brown adipose tissue in healthy men. *N. Engl. J. Med.* 360, 1500–1508
11. Bartelt, A., Bruns, O. T., Reimer, R., Hohenberg, H., Ittrich, H., Peldschus, K., Kaul, M. G., Tromsdorf, U. I., Weller, H., Waurisch, C., Eychmüller, A., Gordts, P. L., Rinninger, F., Bruegelmann, K., Freund, B., Nielsen, P., Merkel, M., and Heeren, J. (2011) Brown adipose tissue activity controls triglyceride clearance. *Nat. Med.* 17, 200–205
12. Ozcan, U., Cao, Q., Yilmaz, E., Lee, A. H., Iwakoshi, N. N., Ozdelen, E., Tuncman, G., Görgün, C., Glimcher, L. H., and Hotamisligil, G. S. (2004) Endoplasmic reticulum stress links obesity, insulin action, and type 2 diabetes. *Science* 306, 457–461
13. Hotamisligil, G. S. (2007) Endoplasmic reticulum stress and inflammation in obesity and type 2 diabetes. *Novartis. Found. Symp.* 286, 86–94
14. Greenberg, A. S., and Obin, M. S. (2006) Obesity and the role of adipose tissue in inflammation and metabolism. *Am. J Clin. Nutr.* 83, 461S-465S
15. Weisberg, S. P., McCann, D., Desai, M., Rosenbaum, M., Leibel, R. L., and Ferrante, A. W., Jr. (2003) Obesity is associated with macrophage accumulation in adipose tissue. *J. Clin. Invest.* 112, 1796–1808
16. Xu, H., Barnes, G. T., Yang, Q., Tan, G., Yang, D., Chou, C. J., Sole, J., Nichols, A., Ross, J. S., Tartaglia, L. A., and Chen, H. (2003) Chronic inflammation in fat plays a crucial role in the development of obesity-related insulin resistance. *J. Clin. Invest.* 112, 1821–1830
17. Shi, H., Kokoeva, M. V., Inouye, K., Tzameli, I., Yin, H., and Flier, J. S. (2006) TLR4 links innate immunity and fatty acid-induced insulin resistance. *J. Clin. Invest.* 116, 3015–3025
18. Tsukumo, D. M., Carvalho-Filho, M. A., Carvalheira, J. B., Prada, P. O., Hirabara, S. M., Schenka, A. A., Araújo, E. P., Vassallo, J., Curi, R., Velloso, L. A., and Saad, M. J. (2007) Loss-of-function mutation in Toll-like receptor 4 prevents diet-induced obesity and insulin resistance. *Diabetes* 56, 1986–1998
19. Pierre, N., Deldicque, L., Barbé, C., Naslain, D., Cani, P. D., and Francaux, M. (2013) Toll-like receptor 4 knockout mice are protected against endoplasmic reticulum stress induced by a high-fat diet. *PLoS One* 8, e65061
20. Kim, F., Pham, M., Luttrell, I., Bannerman, D. D., Tupper, J., Thaler, J., Hawn, T. R., Raines, E. W., and Schwartz, M. W. (2007) Toll-like receptor-4 mediates vascular inflammation and insulin resistance in diet-induced obesity. *Circ. Res.* 100, 1589–1596
21. Crane, J. D., Mottillo, E. P., Farncombe, T. H., Morrison, K. M., and Steinberg, G. R. (2014) A standardized infrared imaging technique that specifically detects UCP1-mediated thermogenesis *in vivo*. *Mol. Metab.* 3, 490–494
22. Okla, M., Ha, J. H., Temel, R. E., and Chung, S. (2015) BMP7 drives human adipogenic stem cells into metabolically active beige adipocytes. *Lipids* 50, 111–120
23. Staszkiewicz, J., Frazier, T. P., Rowan, B. G., Bunnell, B. A., Chiu, E. S., Gimble, J. M., and Gawronska-Kozak, B. (2010) Cell growth characteristics, differentiation frequency, and immunophenotype of adult ear mesenchymal stem cells. *Stem Cells Dev.* 19, 83–92
24. Gawronska-Kozak, B. (2014) Preparation and differentiation of mesenchymal stem cells from ears of adult mice. *Methods Enzymol.* 538, 1–13
25. Lagouge, M., Argmann, C., Gerhart-Hines, Z., Meziane, H., Lerin, C., Daussin, F., Messadeq, N., Milne, J., Lambert, P., Elliott, P., Geny, B., Laakso, M., Puigserver, P., and Auwerx, J. (2006) Resveratrol improves mitochondrial function and protects against metabolic disease by activating SIRT1 and PGC-1alpha. *Cell* 127, 1109–1122
26. Cani, P. D., Amar, J., Iglesias, M. A., Poggi, M., Knauf, C., Bastelica, D., Neyrinck, A. M., Fava, F., Tuohy, K. M., Chabo, C., Waget, A., Delmée, E., Cousin, B., Sulpice, T., Chamontin, B., Ferrières, J., Tanti, J. F., Gibson, G. R., Casteilla, L., Delzenne, N. M., Alessi, M. C., and Burcelin, R. (2007) Metabolic endotoxemia initiates obesity and insulin resistance. *Diabetes* 56, 1761–1772
27. Basseri, S., Lhoták, S., Sharma, A. M., and Austin, R. C. (2009) The chemical chaperone 4-phenylbutyrate inhibits adipogenesis by modulating the unfolded protein response. *J. Lipid Res.* 50, 2486–2501
28. Heinonen, S., Buzkova, J., Muniandy, M., Kaksonen, R., Ollikainen, M., Ismail, K., Hakkarainen, A., Lundbom, J., Lundbom, N., Vuolteenaho, K., Moilanen, E., Kaprio, J., Rissanen, A., Suomalainen, A., and Pietiläinen, K. H. (2015) Impaired mitochondrial biogenesis in adipose tissue in acquired obesity. *Diabetes* 64, 3135–3145
29. Bae, J., Chen, J., and Zhao, L. (2015) Chronic activation of pattern recognition receptors suppresses brown adipogenesis of multipotent mesodermal stem cells and brown pre-adipocytes. *Biochem. Cell Biol.* 93, 251–261

30. Kajimura, S., Seale, P., and Spiegelman, B. M. (2010) Transcriptional control of brown fat development. *Cell Metab.* 11, 257–262
31. Kawasaki, N., Asada, R., Saito, A., Kanemoto, S., and Imaizumi, K. (2012) Obesity-induced endoplasmic reticulum stress causes chronic inflammation in adipose tissue. *Sci. Rep.* 2, 799
32. Rabinowitz, J. D., and White, E. (2010) Autophagy and metabolism. *Science* 330, 1344–1348
33. Singh, R., Xiang, Y., Wang, Y., Baikati, K., Cuervo, A. M., Luu, Y. K., Tang, Y., Pessin, J. E., Schwartz, G. J., and Czaja, M. J. (2009) Autophagy regulates adipose mass and differentiation in mice. *J. Clin. Invest.* 119, 3329–3339
34. Zhang, Y., Goldman, S., Baerga, R., Zhao, Y., Komatsu, M., and Jin, S. (2009) Adipose-specific deletion of autophagy-related gene 7 (atg7) in mice reveals a role in adipogenesis. *Proc. Natl. Acad. Sci. U.S.A.* 106, 19860–19865
35. Jansen, H. J., van Essen, P., Koenen, T., Joosten, L. A., Netea, M. G., Tack, C. J., and Stienstra, R. (2012) Autophagy activity is upregulated in adipose tissue of obese individuals and modulates proinflammatory cytokine expression. *Endocrinology* 153, 5866–5874
36. Kovsan, J., Blüher, M., Tarnovscki, T., Klöting, N., Kirshtein, B., Madar, L., Shai, I., Golan, R., Harman-Boehm, I., Schön, M. R., Greenberg, A. S., Elazar, Z., Bashan, N., and Rudich, A. (2011) Altered autophagy in human adipose tissues in obesity. *J. Clin. Endocrinol. Metab.* 96, E268–E277
37. Nunez, C. E., Rodrigues, V. S., Gomes, F. S., Moura, R. F., Victorio, S. C., Bombassaro, B., Chaim, E. A., Pareja, J. C., Geloneze, B., Velloso, L. A., and Araujo, E. P. (2013) Defective regulation of adipose tissue autophagy in obesity. *Int. J. Obes. (Lond)* 37, 1473–1480
38. Maris, M., Overbergh, L., Gysemans, C., Waget, A., Cardozo, A. K., Verdrengh, E., Cunha, J. P., Gotoh, T., Cnop, M., Eizirik, D. L., Burcelin, R., and Mathieu, C. (2012) Deletion of C/EBP homologous protein (Chop) in C57Bl/6 mice dissociates obesity from insulin resistance. *Diabetologia* 55, 1167–1178
39. Lumeng, C. N., Bodzin, J. L., and Saltiel, A. R. (2007) Obesity induces a phenotypic switch in adipose tissue macrophage polarization. *J. Clin. Invest.* 117, 175–184
40. Nguyen, K. D., Qiu, Y., Cui, X., Goh, Y. P., Mwangi, J., David, T., Mukundan, L., Brombacher, F., Locksley, R. M., and Chawla, A. (2011) Alternatively activated macrophages produce catecholamines to sustain adaptive thermogenesis. *Nature* 480, 104–108
41. Sakamoto, T., Takahashi, N., Sawaragi, Y., Naknukool, S., Yu, R., Goto, T., and Kawada, T. (2013) Inflammation induced by RAW macrophages suppresses UCP1 mRNA induction via ERK activation in 10T1/2 adipocytes. *Am. J. Physiol. Cell Physiol.* 304, C729–C738
42. Wen, H., Gris, D., Lei, Y., Jha, S., Zhang, L., Huang, M. T., Brickey, W. J., and Ting, J. P. (2011) Fatty acid-induced NLRP3-ASC inflammasome activation interferes with insulin signaling. *Nat. Immunol.* 12, 408–415
43. Valdearcos, M., Xu, A. W., and Koliwad, S. K. (2015) Hypothalamic inflammation in the control of metabolic function. *Annu. Rev. Physiol.* 77, 131–160
44. Arruda, A. P., Milanski, M., Coope, A., Torsoni, A. S., Ropelle, E., Carvalho, D. P., Carvalheira, J. B., and Velloso, L. A. (2011) Low-grade hypothalamic inflammation leads to defective thermogenesis, insulin resistance, and impaired insulin secretion. *Endocrinology* 152, 1314–1326
45. Lee, P., Linderman, J. D., Smith, S., Brychta, R. J., Wang, J., Idelson, C., Perron, R. M., Werner, C. D., Phan, G. Q., Kammula, U. S., Kebebew, E., Pacak, K., Chen, K. Y., and Celi, F. S. (2014) Irisin and FGF21 are cold-induced endocrine activators of brown fat function in humans. *Cell Metab.* 19, 302–309
46. Liu, X., Wang, S., You, Y., Meng, M., Zheng, Z., Dong, M., Lin, J., Zhao, Q., Zhang, C., Yuan, X., Hu, T., Liu, L., Huang, Y., Zhang, L., Wang, D., Zhan, J., Jong Lee, H., Speakman, J. R., and Jin, W. (2015) Brown adipose tissue transplantation reverses obesity in Ob/Ob mice. *Endocrinology* 156, 2461–2469
47. Stanford, K. I., Middelbeek, R. J., Townsend, K. L., An, D., Nygaard, E. B., Hitchcox, K. M., Markan, K. R., Nakano, K., Hirshman, M. F., Tseng, Y. H., and Goodyear, L. J. (2013) Brown adipose tissue regulates glucose homeostasis and insulin sensitivity. *J. Clin. Invest.* 123, 215–223
48. Vosselman, M. J., van der Lans, A. A., Brans, B., Wierts, R., van Baak, M. A., Schrauwen, P., and van Marken Lichtenbelt, W. D. (2012) Systemic β-adrenergic stimulation of thermogenesis is not accompanied by brown adipose tissue activity in humans. *Diabetes* 61, 3106–3113
49. Cypess, A. M., Chen, Y. C., Sze, C., Wang, K., English, J., Chan, O., Holman, A. R., Tal, I., Palmer, M. R., Kolodny, G. M., and Kahn, C. R. (2012) Cold but not sympathomimetics activates human brown adipose tissue *in vivo*. *Proc. Natl. Acad. Sci. U.S.A.* 109, 10001–10005